HAL open science

On the Inertia Effects on the Darcy Law: Numerical Implementation and Confrontation of Micromechanics-Based Approaches

Viet-Thanh To, Quy-Dong To, Vincent Monchiet

▶ **To cite this version:**

Viet-Thanh To, Quy-Dong To, Vincent Monchiet. On the Inertia Effects on the Darcy Law: Numerical Implementation and Confrontation of Micromechanics-Based Approaches. Transport in Porous Media, 2016, 111, 10.1007/s11242-015-0588-4 . hal-01329419

HAL Id: hal-01329419

https://hal.science/hal-01329419v1

Submitted on 1 Nov 2023

HAL is a multi-disciplinary open access archive for the deposit and dissemination of scientific research documents, whether they are published or not. The documents may come from teaching and research institutions in France or abroad, or from public or private research centers.

L'archive ouverte pluridisciplinaire **HAL**, est destinée au dépôt et à la diffusion de documents scientifiques de niveau recherche, publiés ou non, émanant des établissements d'enseignement et de recherche français ou étrangers, des laboratoires publics ou privés.

On the inertia effects on the Darcy law: numerical implementation and confrontation of micromechanics-based approaches

Viet-Thanh To · Quy-Dong To · Vincent Monchiet

Abstract In this paper, we investigate the nonlinear deviation of the Darcy law in the domain of high pressure gradient. Classically, the (linear) Darcy law can be deduced from asymptotic homogenization approaches and the numerical resolution of the Stokes flow problem on the unit cell of the porous medium. At higher speed steady flow of a fluid, non linear effects on the macroscopic filtration law arises and are accounted by considering the convection term in the Navier Stokes equation. These non linear effects has been often studied in asymptotic homogenization framework by expanding the solution in power series at low Reynolds number. This has two advantages : (i) the Navier-Stokes problems is replaced by a chain of linear problems with source terms which depend on the solution at lower order, (ii) the macroscopic non linear filtration law is derived in the form of a polynom. We develop a Fast Fourier Transform (FFT) based numerical algorithm to compute the solution of this elementary problems and to compute the higher order permeability tensors in connection with the morphology of the porous medium. The results are then compared to the solution of the full Navier-Stokes problem by means of Finite Element Method (FEM) which allows to evaluate the capacity of the expansion method to account for the non linear effects. We determine the convergence radius of the polynomial series and we give the limit of the series expansion method in term of the Reynolds number.

Keywords Darcy · Forchheimer · inertial effects · homogenization · polynomial law

Viet-Thanh To · Quy-Dong To · Vincent Monchiet
Université Paris-Est, Laboratoire Modélisation et Simulation Multi Echelle, LMSME UMR8208 CNRS, 5 boulevard Descartes, 77454 Marne la Vallée Cedex, France
E-mail: vincent.monchiet@u-pem.fr

Accepted Manuscript

1 Introduction

The determination of permeability in connection with microstructure parameters has been already addressed in the framework of upscaling approaches. Among the firsts, Auriault and Sanchez-Palencia 1977, Sanchez Palencia 1980, Levy 1983, etc. have provided a physical justification of the famous Darcy's Law [11] in framework of periodic homogenization based on matched asymptotic series expansion techniques. The Darcy law gives the flow velocity as a linear function of the applied gradient of pressure and introduces the permeability tensor that is characteristic of the porous material. Moreover, the asymptotic approach also provides the elementary cell problems which has to be solved for computing the permeability. The Darcy law typically reads (for one dimensional problem):

$$V = -\frac{K}{\mu} G \tag{1}$$

where V is the macroscopic velocity, μ the dynamic viscosity characteristic of the fluid, G is the macroscopic pressure gradient and K is the permeability that is characteristic of the morphology of the microstructure. Mentioned must be made of other homogenization approaches based on energy principle and volume averaging (Whitaker [36], Allaire [3], etc).
Many years after Darcy's historical experiment, other researchers found that some deviation from the above-mentioned proportionality law occurs when the velocity increases. As the Reynolds number increases, nonlinearities due to inertia appear. For higher Reynolds numbers, the flow becomes turbulent. Some experimental data for geometrically simple media (see for example Chauveteau and Thirriot [10] or Skjetne et al. [32]) proved the existence of four regimes: (i) Darcy, (ii) Weak inertia (iii) Strong inertia, and (iv) Turbulence. In the domain of weak inertia the Forchheimer [15] law is generally used, it introduces a quadratic term in the velocity field in order to account for the non linear dependence with the applied gradient of pressure and reads:

$$V + \alpha V^2 = -\frac{K}{\mu} G \tag{2}$$

in which αV^2 is the corrective term to the linear Darcy law. Note however that Forchheimer's law was originally postulated but not derived in a homogenization approach. The Forchheimer equation has been found to reproduce adequately various experimental data [20, 34, 2] but fails as regards to other work [10, 17] which suggests to use other formula for the non linear filtration law. For instance, a cubic correction to the Darcy law can be used,

$$V + \beta V^3 = -\frac{K}{\mu} G \tag{3}$$

that is more in agreement with the recent experimental data provided by Zermatten et al. [38]. Note also that numerical simulations with the Finite

Accepted Manuscript

Element Method (FEM) has been performed in order to validate or not some macroscopic models of filtration (see for instance [14] and [19]).
Various contributions have been proposed to provide a physical basis for the Forchheimer law or to derive more general non linear equations in order to physically explain the origin of non linear effect in the "weakly non linear" regime. Particularly, still in the framework of periodic homogenization based on matched asymptotic series, various authors developed a non linear filtration law for porous media starting from the stationary Navier-Stokes equation among which Mei and Auriault [22], Wodie and Levy [37], Giorgi [16], Skjetne and Auriault [33], Chen et al. [9], Bahloff et al. [6]. The Darcy law is recovered by keeping the first order term in the expansion series, the non linear effects are captured by accounting for higher order terms. Particularly, in Refs.[22, 37, 31, 33], the authors found results which are much different from Forchheimer equation. Indeed, the second order term of the expansion series is null and the third order term introduces a correction to Darcy's law that is cubic. By keeping all the terms of the expansion series, the filtration law is of polynomial type in which the quadratic term is null. Each tensors of this law can be computed from numerical calculation of successive Stokes-type problem at the local scale which is much simpler and faster than solving the full Navier-Stokes equations. Unlike previous works [22, 37, 33], Chen et al. [9] showed that the first correction to Darcy law is quadratic. They also use the asymptotic series expansion method but with different scaling assumptions. Note that the need to obtain a quadratic term in the macroscopic filtration law was motivated by earlier experimental data [23]. However, a dependence with a quadratic term at low Reynolds number has not been reported by the recent numerical computations based on the resolution of the full Navier-Stokes equations at the microscopic scale [30, 6, 1]. Particularly, in Ref. [1], the authors suggests that there is no quadratic term at low Reynolds number but an approximation of the macroscopic non linear Darcy law at higher Reynolds number could includes a quadratic term. The comparison between the polynomial approximate filtration law obtained from asymptotic homogenization approach with the solution of full Navier Stokes problem has been recently studied by Bahloff et al. [6] in the case of the flow through a periodic axisymmetric sinusoidal channel and by Adler et al. [1] for the problem of flow between two wavy walls and for which, in each cases, the macroscopic model is one-dimensional.
It can be shown that the homogenization approach used to derive the non-linear filtration law involves the resolution of periodic Navier-Stokes fluid flow in the unit cell under an applied pressure gradient. This equivalence is only valid if we solve and superpose infinitely the hierarchy of Stokes problems in the unit cell, which is numerically impossible. It is noted that when the latter approach is employed for a finite number of times, the polynomial filtration law can be obtained, as done by many previous works [6, 1]. In order to assess the accuracy of polynomial law, we exploit the aforementioned equivalence and compare the homogenization solutions with the exact one issued from Finite Element Method. We have developed a new Fast Fourier Transform scheme to deal with the periodic homogenization problem and use COMSOL to obtain

Accepted Manuscript

the exact solution. The microstructure under consideration constituted of 2D aligned cylinders with circular and rectangular cross sections. The obtained results are surprisingly interesting. It is found that the polynomial laws only provide small corrections to the linear Darcy law while they are only valid for a finite range of the pore Reynolds number $\mathcal{R}_e$ and still deviate at high values of $\mathcal{R}_e$. These numerical evidences suggest that non-polynomial filtration law should be used to extend the validity to high $\mathcal{R}_e$ range. These results briefly summarize the notable contribution of the present works. The details of the paper are organized in section as follows. In section 2, we recall the principle of the expansion series method, we provide the hierarchy of unit cell problems which have to be solved for computing the permeability tensors of the polynomial macroscopic filtration law. In section 3, we provides a FFT based numerical approach to compute the solution of the chain of cell problems and the permeability tensors at different orders. In section 4, numerical applications for 2d microstructures constituted of aligned cylinders. The polynomial approximate filtration law is compared with a reference solution obtained by computing the full Navier-Stokes problem with finite elements. In order to evaluate accurately the limit of the series expansion method, we determine the convergence radius of the polynomial series and we provide the limite for the pore Reynolds Number.

2 Approximation with series expansion method

We consider a periodic porous medium saturated by a homogeneous Newtonian viscous fluid with the dynamic viscosity μ. By V, we denote the total volume of the cell, by V_f and V_s the volume occupied by the fluid and the solid respectively. The frontier between the fluid and the solid is denoted S.

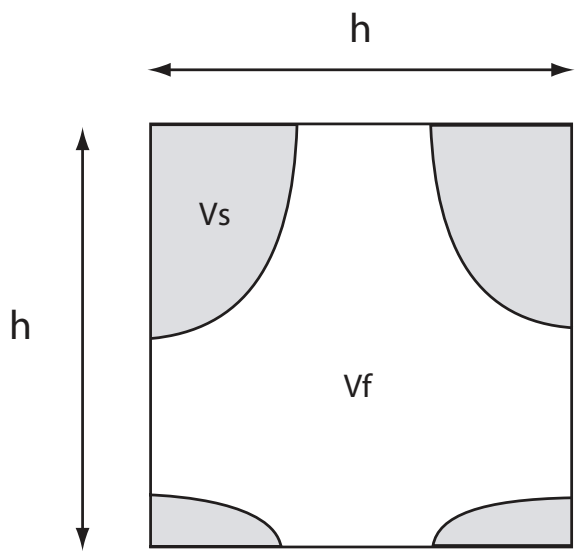

Fig. 1 Periodic unit cell of the porous medium.

Accepted Manuscript

We consider, within the unit cell, the Navier-Stokes problem under an applied pressure gradient $\boldsymbol{G}$:

$$\begin{aligned} \mu \Delta \boldsymbol{v} - \nabla p - \boldsymbol{G} = \rho(\nabla \boldsymbol{v}).\boldsymbol{v} \quad & \text{in } V_f \\ \operatorname{div} \boldsymbol{v} = 0 \quad & \text{in } V_f \\ \boldsymbol{v} = 0 \quad & \text{in } S \end{aligned} \tag{4}$$

with the periodicity conditions for the velocity and the pressure:

$$\boldsymbol{v} \text{ periodic}, \quad p \text{ periodic} \tag{5}$$

In (4), μ and ρ are respectively the dynamic viscosity and density, Δ, ∇ and div are the laplacian, gradient and divergence operator. The first and second relations in (4) are the momentum equation and incompressibility condition and the last equation is the non slip condition on the interface S between the fluid and the solid.
We seek for the relation giving the macroscopic velocity $\boldsymbol{V}$ as function of the applied pressure gradient $\boldsymbol{G}$. In order to obtain results independently of the values of fluid characteristics, ρ and μ, and on the size of the unit cell h, it is suitable to use the following change of variables:

$$\boldsymbol{v} = \boldsymbol{v}^* \frac{\mu}{\rho h}, \quad p = p^* \frac{\mu^2}{\rho h^2}, \quad \boldsymbol{G} = \frac{\mu^2}{\rho h^3} \boldsymbol{J}, \quad \nabla = \frac{1}{h} \nabla^* \tag{6}$$

Introducing these non dimensional parameters in (4) yields to:

$$\begin{aligned} \Delta^* \boldsymbol{v}^* - \nabla^* p^* - \boldsymbol{J} = (\nabla^* \boldsymbol{v}^*).\boldsymbol{v}^* \quad & \text{in } V_f^* \\ \operatorname{div}^* \boldsymbol{v}^* = 0 \quad & \text{in } V_f^* \\ \boldsymbol{v}^* = 0 \quad & \text{in } S^* \end{aligned} \tag{7}$$

The mean velocity field computed over the volume V of the unit cell can be put into the following form:

$$\boldsymbol{V}^* = < \boldsymbol{v}^* >_V = \mathcal{F}(\boldsymbol{J}) \tag{8}$$

in which $\mathcal{F} : \boldsymbol{J} \to \mathcal{F}(\boldsymbol{J})$ is an unknown non linear function of the variable $\boldsymbol{J}$. The macroscopic filtration law for physical variables $\boldsymbol{V}$ and $\boldsymbol{G}$ is:

$$\boldsymbol{V} = \frac{\mu}{\rho h} \mathcal{F} \left(\frac{\rho h^3}{\mu^2} \boldsymbol{G} \right) \tag{9}$$

At low speed steady flow of a fluid in the porous medium, the term at the right side of the equality in (7) can be neglected and the solution linearly depends on the applied pressure gradient. In this context, the macroscopic description of the fluid flow through the porous solid is the Darcy law. As speed increases, the nonlinear inertial terms grow and the flow law becomes nonlinear.
The approximation of the macroscopic filtration law at low pore Reynolds number has been investigated by several authors among which Mei and Auriault [22], Wodie and Levy [37], Firdaous et al. [14], Skjetne and Auriault [33],

Accepted Manuscript

Chen et al. [9], Bahloff et al. [6], Adler et al. [1]. Let us briefly recall the main results obtained by these authors. Consider the following change of variables:

$$\boldsymbol{v} = v_c\overline{\boldsymbol{v}}, \quad p = \frac{\mu v_c}{h}\overline{p}, \quad \boldsymbol{G} = \frac{\mu v_c}{h^2}\overline{\boldsymbol{G}}, \quad \nabla = \frac{1}{h}\nabla^* \tag{10}$$

in the Navier-Stokes problem (4), where $v_c = \|\boldsymbol{V}\|$ is the characteristic velocity, chosen as the norm of the macroscopic velocity field following [19]. Introducing also the pore Reynolds number:

$$\mathcal{R}_e = \frac{\rho v_c h}{\mu} \tag{11}$$

we obtain the following alternative form for the Navier-Stokes equations (4):

$$\begin{aligned} \Delta^*\overline{\boldsymbol{v}} - \nabla^*\overline{p} - \overline{\boldsymbol{G}} = \mathcal{R}_e(\nabla^*\overline{\boldsymbol{v}}).\overline{\boldsymbol{v}} \quad & \text{in } V_f^* \\ \operatorname{div}^*\overline{\boldsymbol{v}} = 0 \quad & \text{in } V_f^* \\ \overline{\boldsymbol{v}} = 0 \quad & \text{in } S^* \end{aligned} \tag{12}$$

Assuming low values of the pore Reynolds number, the solution is searched as a power series in $\mathcal{R}_e$:

$$\begin{aligned} \overline{\boldsymbol{v}} &= \boldsymbol{v}^0 + \mathcal{R}_e\boldsymbol{v}^1 + \mathcal{R}_e^2\boldsymbol{v}^2 + \mathcal{R}_e^3\boldsymbol{v}^3 ... \\ \overline{p} &= p^0 + \mathcal{R}_e p + \mathcal{R}_e^2 p^2 + \mathcal{R}_e^3 p^3 ... \end{aligned} \tag{13}$$

Introducing expressions (13) in the system (12) and collecting all the terms having the same power in $\mathcal{R}_e$ leads to a hierarchy of cell problems.
The first order unit cell problem is classic in homogenization of porous media and provides the macroscopic Darcy law. This problem reads:

$$\Delta^*\boldsymbol{v}^0 - \nabla^* p^0 - \overline{\boldsymbol{G}} = 0, \quad \operatorname{div}^*(\boldsymbol{v}^0) = 0 \tag{14}$$

This is a linear problem for $\boldsymbol{v}^0$ and p^0. The solution reads:

$$v_i^0 = A_{ij}^0\overline{G}_j, \quad p^0 = B_i^0\overline{G}_i \tag{15}$$

where A_{ij}^0 and B_i^0 are two localization tensor which depends on the coordinates $\boldsymbol{x}$ and which are determined by solving the elementary problem (14) with the periodicity condition on its boundary and the adherence condition on ∂V_f.
All higher order problems can be read in the compact form:

$$\Delta^*\mathbf{v}^n - \nabla^* p^n = \sum_{k=0}^{k=n-1} \nabla^*\boldsymbol{v}^{n-1-k}.\boldsymbol{v}^k \tag{16}$$

and the solution is:

$$v_i^n = A_{ij...p}^n\overline{G}_j...\overline{G}_p, \quad p^n = B_{j...q}^n\overline{G}_j..\overline{G}_p \tag{17}$$

Each cell problems and each associated localization tensors ($A_{ij...p}^n$ and $B_{j...q}^n$) only depends on the geometry of the unit cell of the porous material. Again,

Accepted Manuscript

the elementary problems (16) are solved with the periodicity condition on the boundary of cell and the adherence condition on ∂V_f.
The total velocity field is obtained from the first relation in (13) together with (15) and (17). This leads to:

$$\overline{v}_i = A^0_{ij}\overline{G}_j + \mathcal{R}_e A^1_{ijk}\overline{G}_j\overline{G}_k + \mathcal{R}_e^2 A^2_{ijkp}\overline{G}_j\overline{G}_k\overline{G}_p + ... \tag{18}$$

The macroscopic velocity is:

$$\overline{V}_i =< \overline{v}_i >_V = -\left[K^0_{ij}\overline{G}_j + \mathcal{R}_e K^1_{ijk}\overline{G}_j\overline{G}_k + \mathcal{R}_e^2 K^2_{ijkp}\overline{G}_j\overline{G}_k\overline{G}_p + ...\right] \tag{19}$$

where K^0_{ij}, K^1_{ijk}, K^2_{ijkp}, K^3_{ijkpq}, are the components of the dimensionless permeability tensors at the different orders, defined by:

$$K^n_{ij..k} = - < A^n_{ij..k} >_V \tag{20}$$

The inversion of the infinite series filtration law is:

$$\overline{G}_i = -\left[H^0_{ij}\overline{V}_j + \mathcal{R}_e H^1_{ijk}\overline{V}_j\overline{V}_k + \mathcal{R}_e^2 H^2_{ijkp}\overline{V}_j\overline{V}_k\overline{V}_p + ...\right] \tag{21}$$

in which H^0_{ij}, H^1_{ijk}, H^2_{ijkp}, H^3_{ijkpq}, are the components of dimensionless hydraulic resistivity tensors. They are obtained by replacing, in (19), $\overline{G}_i$ by (21) and by collecting all the terms having the same power in V_i:

$$\overline{V}_i = \left[K^0_{ij}H^0_{jp}\right]\overline{V}_p + \left[K^0_{ij}H^1_{jpq} + K^1_{ijk}H^0_{jp}H^0_{kq}\right]\overline{V}_p\overline{V}_q + ... \tag{22}$$

In the above relation, the first term at the right of the equality must be equal to V_i^* and all other terms must be equal to zero. This leads to a set of linear equations for which H^0_{ij}, H^1_{ijk}, ... are the unknowns:

$$\begin{aligned} &K^0_{ip}H^0_{pj} = \delta_{ij} \\ &K^0_{ip}H^1_{pjk} + K^1_{ipq}H^0_{pj}H^0_{qk} = 0 \\ &... \end{aligned} \tag{23}$$

and which must be solved successively to obtain the hydraulic resistivity tensors. With the re-normalization of the quantities, the polynomial filtration law is:

$$V_i = -\frac{h^2}{\mu}\left[K^0_{ij}G_j + \frac{\rho h^3}{\mu^2}K^1_{ijk}G_jG_k + \left(\frac{\rho h^3}{\mu^2}\right)^2 K^2_{ijkp}G_jG_kG_p + ...\right] \tag{24}$$

The first term is the Darcy law, the higher order terms appears as corrections to the linear approximation. By doing the same in equation (21), one obtains:

$$G_i = -\frac{\mu}{h^2}\left[H^0_{ij}V_j + \frac{\rho h}{\mu}H^1_{ijk}V_jV_k + \left(\frac{\rho h}{\mu}\right)^2 K^2_{ijkp}V_jV_kV_p + ...\right] \tag{25}$$

Let us now introduce the change of variables (6) in relation (24), it gives:

$$V_i^* = -\left[K^0_{ij}J_j + K^1_{ijk}J_jJ_k + K^2_{ijkp}J_jJ_kJ_p + ...\right] \tag{26}$$

Accepted Manuscript

which, comparing with equation (8), leads to a polynomial expression for the function $\mathcal{F}(\boldsymbol{J})$. In order to investigate the deviation between the polynomial approximation and the exact solution of Navier-Stokes problem it is more convenient to use the set of dimensionless variables $(\boldsymbol{V}^*, \boldsymbol{J})$ since the relations (8) and (26) are independent of the size of the unit cell, of the nature of the fluid and the Reynolds number. Also, it must be noted from equation (10) that:

$$v_c = \|\boldsymbol{V}\| = \frac{\mu}{\rho h}\|\boldsymbol{V}^*\| \tag{27}$$

which, introduced in (11), gives:

$$\mathcal{R}_e = \|\boldsymbol{V}^*\| \tag{28}$$

Which is important for the interpretation of the numerical results in term of the pore Reynolds number.
All the permeability tensors are computed by solving the elementary problems which are described in equations (15) and (17). The comparison between the polynomial approximation and the full solution obtained by the resolution of the Navier-Stokes equation has been provided in two cases: the fluid flow between two wavy walls have been studied by [1] and the solution for the flow in a periodic axisymmetric sinusoidal channel has been numerically computed by [6]. Alternatively, the implementation of Navier-Stokes problem (7) for various porous microstructures can be found for example in [14] but the results have not been compared with the polynomial approximation derived from the resolution of the chain of elementary cell problems (15) and (17). The computation of the higher order permeability tensor has never been computed in the case of an array of periodic array of cylinders, that is of great importance to evaluate the capacity if the expansion series method to reproduce the non linear effects and to determine the limit of the approach.
The first correction to Darcy law has been proved in [22] to cancel out. This is obviously trivial when considering a unit cell having plane symmetries, since all the tensors of odd number vanishes. However this result has been demonstrated in [14,33] for arbitrary anisotropic porous media. The correction in the Darcy law can then be found in the cubic term. This suggests that the Forchheimer law, which introduces a quadratic corrective term, is not in agreement with the results of the homogenization approach. This result was also supported by various numerical results [7,14,32]. The accuracy and range of validity of the correction terms of Darcy law must be evaluated by (i) computing higher order terms of the series (ii) by making the comparison with the full resolution of Navier Stokes problem. In the next section we propose a suitable FFT based numerical algorithm to compute the solution of cell problems at any order and the computation of the associated permeability tensors. The comparisons with the FEM solutions of the Navier Stokes problem are presented for various applications in section 4.

Accepted Manuscript

3 Resolution of cell problems with FFT

The FFT method, which have been introduced for linear elastic composite has been adapted in [25,29] to handle the problem of Stokes flow through a rigid skeleton due to a prescribed pressure gradient. This method has computational advantages since its is very fast and the memory requirement is strongly reduced compared to FEM that is obvious of great interest for applications to complex 3d microstructures [21]. In this section we extend this iterative scheme to deal with higher order cell problems.
Each one can be formally written as a Stokes problem in the presence of a source term denoted $\boldsymbol{f}$:

$$\begin{aligned} \Delta^* \boldsymbol{v}^* - \nabla^* p^* - \boldsymbol{f} = 0 \quad & \text{in} V_f^* \\ \text{div}^* \boldsymbol{v}^* = 0 \quad & \text{in} V_f^* \\ \boldsymbol{v}^* = 0 \quad & \text{in} V_s^* \end{aligned} \tag{29}$$

in which $\boldsymbol{f}$ is given by:

$$\boldsymbol{f} = \boldsymbol{J} \tag{30}$$

in the fluid phase and for the first order problem. For higher order cell problems, the source term is given by:

$$\boldsymbol{f} = \sum_{k=0}^{k=n-1} \nabla^* \boldsymbol{v}^{n-1-k}.\boldsymbol{v}^k \tag{31}$$

in the fluid phase. Expression of $\boldsymbol{f}$ in the solid phase will be specified in the next of this section. In the system of equations (29), we make a continuation by continuity of the fields within the solid phase that is required when using the FFT method. Classically, when using FEM, only the fluid phase is meshed and a null velocity at the interface with the solid is considered as boundary conditions. However, the method of resolution based on FFT techniques uses Fourier series discretization which are defined at any points within the unit cell. The condition $\boldsymbol{v} = 0 \in V_s$ is recovered by introducing, in the solid phase, a fictitious dynamic viscosity that is very large and which can be interpreted as a penalty coefficient.
Since all the cell problems are formally equivalent when introducing $\boldsymbol{f}$, the iterative scheme used in [25] can be also considered for solving higher order cell problems. This iterative scheme reads:

$$\widehat{\boldsymbol{\sigma}}^{i+1} = \widehat{\boldsymbol{\sigma}}^i - \widehat{\boldsymbol{\Delta}}^0 : \widehat{\boldsymbol{d}}^i \tag{32}$$

where $\widehat{\boldsymbol{\sigma}}$ is the stress tensor (and $\widehat{\boldsymbol{\sigma}}$ denotes its Fourier transform) defined by

$$\boldsymbol{\sigma} = 2\mu(x)\boldsymbol{d} - p\boldsymbol{I}, \quad \boldsymbol{d} = \frac{1}{2}(\nabla \boldsymbol{v}^* + \nabla^T \boldsymbol{v}^*) \tag{33}$$

Accepted Manuscript

in which $\mu(x)$ defined by :

$$\mu(x) = \begin{cases} 1 \text{ in } V_f^* \\ q \text{ in } V_s^* \end{cases} \tag{34}$$

where q is the penalty coefficient chosen sufficient large to retrieve the condition $\boldsymbol{v} = 0$ with the solid phase. By inversion, the Fourier transform of the strain rate tensor, computed at iteration i, reads:

$$\widehat{\boldsymbol{d}}^i = \left[\frac{1}{2}\widehat{\mathrm{I}}_f + \frac{1}{2q}\widehat{\mathrm{I}}_s\right] * \left[\boldsymbol{\sigma}^i - p^i\boldsymbol{I}\right] \tag{35}$$

where $\widehat{I}_f$ and $\widehat{I}_s$ are the Fourier transform of the characteristic function of the fluid and the solid phase:

$$\mathrm{I}_f = \begin{cases} 0 \text{ in } V_s \\ 1 \text{ in } V_f \end{cases} \quad \mathrm{I}_f = 1 - \mathrm{I}_s \tag{36}$$

In our computation, the value $1/q = 0$ can be considered with a good convergence of the iterative scheme.
The iterative scheme also uses the complementary Green operator $\boldsymbol{\Delta}^0$ for an incompressible homogeneous medium of dynamic viscosity μ_0 defined by:

$$\widehat{\boldsymbol{\Delta}}^0 = 2\mu_0\left[\boldsymbol{k}^\perp \otimes \boldsymbol{k}^\perp + \boldsymbol{k}^\perp \underline{\overline{\otimes}} \boldsymbol{k}^\perp\right] \tag{37}$$

for $\boldsymbol{\xi} \neq 0$ and $\widehat{\boldsymbol{\Delta}}^0 = 0$ for $\boldsymbol{\xi} = 0$ and where $\boldsymbol{k}$ and $\boldsymbol{k}^\perp$ are given by:

$$\boldsymbol{k} = \frac{1}{|\boldsymbol{\xi}|^2}\boldsymbol{\xi} \otimes \boldsymbol{\xi}, \qquad \boldsymbol{k}^\perp = \boldsymbol{I} - \boldsymbol{k} \tag{38}$$

and $\boldsymbol{I}$ is the two order identity tensor.
The iterative scheme (32) is initialized with :

$$\widehat{\boldsymbol{\sigma}}^{i=1} = -\boldsymbol{\Omega}.\widehat{\boldsymbol{f}} \tag{39}$$

where the components of $\boldsymbol{\Omega}$ are also explicit in the Fourier space:

$$\Omega_{ijk}(\boldsymbol{\xi}) = \frac{i}{\|\boldsymbol{\xi}\|}[\delta_{ij}\overline{\xi}_k + \delta_{ik}\overline{\xi}_j + \delta_{jk}\overline{\xi}_i - 2\overline{\xi}_i\overline{\xi}_j\overline{\xi}_k], \overline{\boldsymbol{\xi}} = \boldsymbol{\xi}/\|\boldsymbol{\xi}\| \tag{40}$$

Once the convergence is achieved, one can compute the velocity field from the strain rate tensor $\widehat{\boldsymbol{d}}$:

$$\widehat{\boldsymbol{v}} = -\frac{2i}{\|\boldsymbol{\xi}\|^2}\widehat{\boldsymbol{d}}.\boldsymbol{\xi}; \forall \boldsymbol{\xi} \neq 0 \tag{41}$$

The velocity field is defined by its Fourier coefficients for any values of $\boldsymbol{\xi}$ except for $\boldsymbol{\xi} = 0$. It means that the velocity field is defined up to an added constant that represents its mean value of the unit cell. This constant is identified by the condition that $\boldsymbol{v} = 0$ in the solid phase.

Accepted Manuscript

Since the stress tensor is antiperiodic on the opposite side of the unit cell, the average of the first equation in (29) leads to:

$$< \boldsymbol{f} >_V = 0 \tag{42}$$

that is the equilibrium of the unit cell. For the first order cell problem, $\boldsymbol{f}$ is equal to $\boldsymbol{J}$ in the fluid phase. In order to comply with the above condition a constant term is introduced in the solid phase. In order to avoid any misunderstanding, we denote by $\boldsymbol{f}_f$ and $\boldsymbol{f}_s$ the value of $\boldsymbol{f}$ taken in the fluid and the solid phase respectively. Their expressions are:

$$\boldsymbol{f}_f = \boldsymbol{J}, \quad \boldsymbol{f}_s = -\frac{c_f}{c_s}\boldsymbol{J} \tag{43}$$

where c_f and c_s denotes the volume fraction of the fluid and solid phase. The term $\boldsymbol{f}_s$ physically represents the drag force due to the flow around the solid phase. Considering now the second order problem, one has:

$$c_s < \boldsymbol{f} >_{V_s} + c_f < \nabla \boldsymbol{v}^0 . \boldsymbol{v}^0 >_{V_f} = 0 \tag{44}$$

Using the divergence theorem, the second integral in the above relation can be split into two surface integrals over the boundary of the cell and the interface with the solid phase:

$$\int_V v^0_{i,j} v^0_j dx = \int_{\partial V_f} v^0_i v^0_j n_j dx + \int_S v^0_i v^0_j n_j dx \tag{45}$$

where ∂V_f is the boundary of the cell crossed by the fluid and S the interface between the solid and the fluid. The integral over ∂V_f is null since $\boldsymbol{v}^0$ is periodic (the term $v^0_j n_j$ is then antiperiodic) and the integral over S is also null due to the adherence condition ($\boldsymbol{v}^0 = 0$ at the solid-fluid interface). It follows that, for the second order problem, the equilibrium condition (42) reduces to $< \boldsymbol{f} >_{V_s} = 0$ which suggests to put $\boldsymbol{f} = 0$ in the solid phase. This result has the following physically interpretation : there is no drag forces in the solid phase for higher order homogenization problems.
This choice is also applicable to all higher order cell problems since in (16) the velocities $\boldsymbol{v}^m$ and $\boldsymbol{v}^{n-m}$ are periodic and null on the surface S.
The numerical integration of the iterative scheme is made using a representation of Fourier transform with a finite number of wave vectors along each space direction. The convolution product in (35) is made by using the FFT algorithm which makes the method very fast. More details about the discretization of the FFT based iterative can be found in [25,29].

4 Application and comparison with FEM solutions

4.1 Presentation of the problem

In this section we applied the method based on FFT to compute the higher order permeability tensor for two particular microstructures made up of aligned

Accepted Manuscript

rigid cylinder having circular and squared crossed sections (see figure 2). The computations are performed on a dimensionless squared domain (whose size is 1 along each space directions) and the solution is carried out by taking a grid 128×128 wave vectors. Both problems are two-dimensional and considering the symmetries of the unit cell, the permeability tensors are cubic in the plane Ox_1x_2. As a consequence, all tensors of odd number vanishes. An approximation at the fifth order then introduces the classic two order permeability tensor $\boldsymbol{K}^0$, also the fourth-order, sixth-order,... tensors.

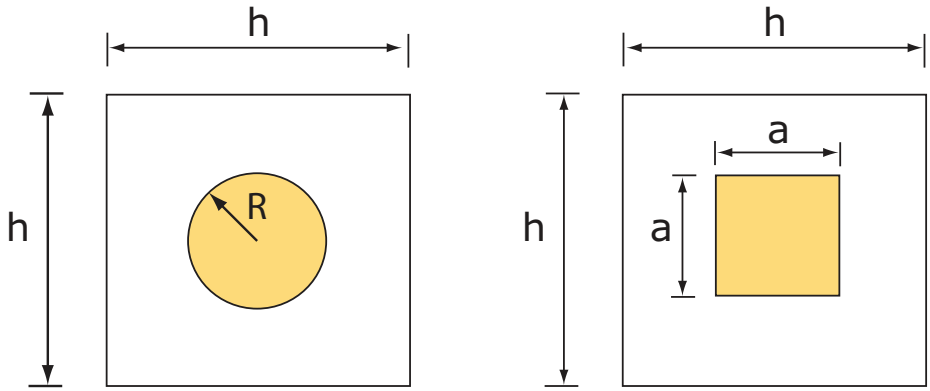

Fig. 2 Periodic unit cell for the arrays of cylinders with crossed and squared sections.

This involves the identification of a large number of coefficients whose number must be reduced by considering the symmetries. The representations in complete forms for tensor functions in two dimensional space has been provided by [39] and are used to provide the irreducible representation of the filtration law. With dimensionless variables, the macroscopic law provides a relation between the normalized macroscopic velocity $\boldsymbol{V}^*$ as function of the applied pressure gradient $\boldsymbol{J}$. For the problem considered in this section, the unit cell is invariant by any rotation of an angle $\theta = \pi/2$ and by the reflection respectively with axes Ox_1 and Ox_2, that corresponding to the class of symmetry C_{4v} with the notation used in [39]. In such case, any non linear vector-valued function can be written into the general form:

$$\boldsymbol{V}(\boldsymbol{J}) = F(I_1, I_2)\boldsymbol{J} + G(I_1, I_2)\boldsymbol{\Pi} \tag{46}$$

in which I_1 and I_2 are the two scalar invariants:

$$I_1 = J_1^2 + J_2^2, \quad I_2 = J_1^2 J_2^2 \tag{47}$$

while $\boldsymbol{\Pi}$ is a vector whose components are:

$$\Pi_i = \begin{pmatrix} J_1^3 \\ J_2^3 \end{pmatrix} \tag{48}$$

Accepted Manuscript

The solution of the unit cell problem (4), without any approximation, is non linear with respect to the applied macroscopic pressure gradient, and the associated filtration law can be put into the general form given by (46). However, in the latter, functions $F(I_1, I_2)$ and $G(I_1, I_2)$ are undetermined. In order to derive the polynomial expression of the macroscopic law, a polynomial expression must then be considered for the two functions $F(I_1, I_2)$ and $G(I_1, I_2)$:

$$F(I_1, I_2) = k_0 + k_2 I_1 + k_4 I_1^2 + k_4' I_2 + k_6 I_1^4 + k_6'' I_1 I_2 + ... \tag{49}$$

$$G(I_1, I_2) = k_2' + k_4'' I_1 + k_6''' I_1^2 + k_6'''' I_2 ... \tag{50}$$

Introducing these expressions in (46) and collecting all the term with the same power in $\boldsymbol{G}$ gives:

$$\begin{aligned}
&\boldsymbol{V}^0(\boldsymbol{J}) = k_0 \boldsymbol{J} \\
&\boldsymbol{V}^1(\boldsymbol{J}) = 0 \\
&\boldsymbol{V}^2(\boldsymbol{J}) = k_2 I_1 \boldsymbol{J} + k_2' \boldsymbol{\Pi} \\
&\boldsymbol{V}^3(\boldsymbol{J}) = 0 \\
&\boldsymbol{V}^4(\boldsymbol{J}) = k_4 I_1^2 \boldsymbol{J} + k_4' I_2 \boldsymbol{J} + k_4'' I_1 \boldsymbol{\Pi} \\
&\boldsymbol{V}^5(\boldsymbol{J}) = 0 \\
&\boldsymbol{V}^6(\boldsymbol{J}) = k_6 I_1^4 \boldsymbol{J} + k_6'' I_1 I_2 \boldsymbol{J} + k_6''' I_1^2 \boldsymbol{\Pi} + k_6'''' I_2 \boldsymbol{\Pi} \\
&...
\end{aligned} \tag{51}$$

When $\boldsymbol{J}$ is oriented along the axis of symmetry (Ox_1 or Ox_2), the velocity field is colinear to $\boldsymbol{J}$. Indeed, consider the particular case corresponding to $J_1 = 1$ and $J_2 = 0$, on observe that the second component of vector $\boldsymbol{\Pi}$, that is given by J_2^3, is null. Consequently, the component V_2 is also null. This result is also true when the $\boldsymbol{J}$ is oriented along the direction Ox_2. Consider now the case of a pressure gradient applied along an arbitrary direction θ, the components of $\boldsymbol{J}$ can then be put in the form:

$$J_1 = \|\boldsymbol{J}\| \cos(\theta), \quad J_2 = \|\boldsymbol{J}\| \sin(\theta) \tag{52}$$

where $\|\boldsymbol{J}\|$ represents the norm of the pressure gradient. Denoting $\boldsymbol{n} = \boldsymbol{J}/\|\boldsymbol{J}\|$ and $\boldsymbol{t}$ the vector orthogonal to $\boldsymbol{n}$, their components are respectively $n_1 = \cos(\theta)$, $n_2 = \sin(\theta)$, $t_1 = -\sin(\theta)$, $t_2 = \cos(\theta)$, and using the non linear relation

$$\mathbf{V}(\mathbf{J}) = F(I_1, I_2)\mathbf{J} + G(I_1, I_2)\boldsymbol{\Pi} \tag{53}$$

we found after some elementary mathematical manipulations:

$$\boldsymbol{V}.\boldsymbol{n} = F(I_1, I_2)\|\boldsymbol{J}\| + G(I_1, I_2)\|\boldsymbol{J}\|^3(\cos^4(\theta) + \sin^4(\theta)) \tag{54}$$

$$\boldsymbol{V}.\boldsymbol{t} = \frac{1}{4} G(I_1, I_2)\|\boldsymbol{J}\|^3 \sin(4\theta) \tag{55}$$

It appears that the fluids flows along the same direction that $\boldsymbol{J}$ if $\theta = 0$, $\theta = \pi/2$ or $\theta = \pi/4$. For all other values of θ, the direction of fluid flow is not

Accepted Manuscript

colinear to the direction of the applied pressure gradient, that is in agreement with the recent results of Lasseux et al. [19].

4.2 Computation of permeability tensors

In the numerical applications provided in this section, the solution is expanded at the fifth order, leadings to the identification of coefficients k_0, k_2, k_2', k_4, k_4' and k_4'' using the FFT algorithm. For instance, the values of these coefficients are provided in table 1 for the case of an array of cylinder with circular crossed section with radius $R = 0.05$, $R = 0.25$ and $R = 0.45$. The variations of the

R	k_0 (10^{-3})	k_2 (10^{-8})	k_2' (10^{-8})	k_4 (10^{-14})	k_4' (10^{-13})	k_4'' (10^{-14})
0.05	133.356	-1.5110^3	1.3310^3	2.0510^5	8.1910^4	-1.8410^5
0.25	19.9045	-3.3531	2.7617	3.3948	1.2469	-2.2710
0.45	0.31852	-9.0510^{-7}	-2.1610^{-6}	4.9010^{-10}	-3.5010^{-10}	8.7910^{-10}

Table 1 Effective permeability coefficients of the polynomial non linear Darcy law for an array of cylinders with circular crossed section with radius R

macroscopic (dimensionless) velocity with the normalized pressure gradient J_1 are provided on figure 3 for the array of cylinders with circular cross section with the radius $R = 0.05$. On this figure, are compared, the first order approximation (the linear Darcy law), the polynomial approximation at the third and fifth order and the finite element solution of the full Navier-Stokes problem. Figures 4, 5 and 6 displays the same results but for the radii $R = 0.25$, $R = 0.45$ and $R = 0.49$. Figure 7 provides the results for a cylinder with rectangular cross section with $a = 0.25$. The FEM data, which are considered as the reference solution since there obtained without any approximations, are used to evaluate the accuracy of the approach based on series expansion. Clearly, the improvement obtained with the third order and the fifth order solution upon the linear approximation is difficult to distinguish on these figures. Indeed, in the range for which the FEM solution differs from the Darcy law, the polynomial approximation fails to reproduce the non linear effects at larger values of $\boldsymbol{J}$.

Furthermore, the use of the third order and the fifth order approximation improve the Darcy at small pressure gradient, however, in this domain the differences between the FEM solution and the linear approximation is very slight. The results show that the polynomial approximation is only applicable for low values of J_1 (or equivalently for low Reynolds number), however, in this range, the correction to Darcy law is not really significant. It must be mentioned that these results are qualitatively similar to that already obtained by

Accepted Manuscript

[6] in the case of the flow through a periodic axisymmetric sinusoidal channel.

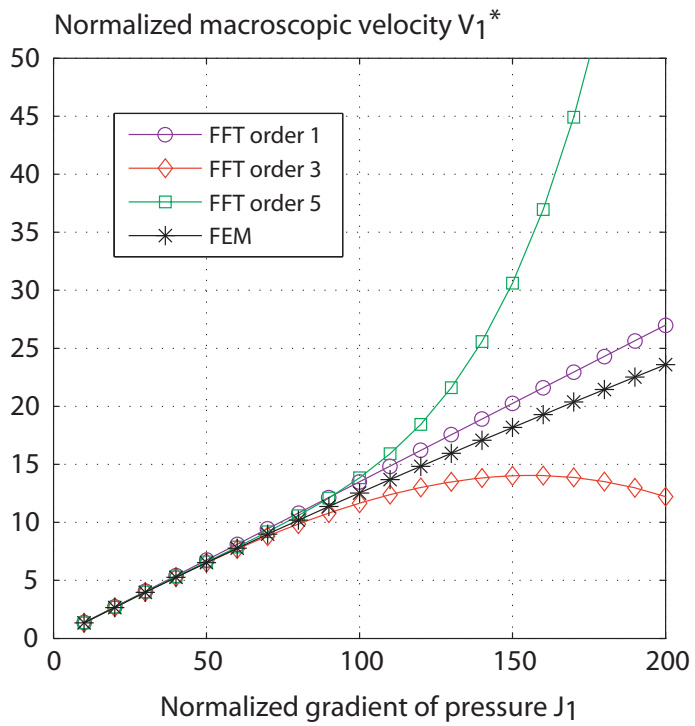

Fig. 3 Variations of the normalized macroscopic velocity V_1^* as function of the normalized macroscopic pressure gradient J_1 for the array of cylinder with circular cross section with radius $R = 0.05$. Comparison between the first order, third order, fifth order approximation and the (FEM based) full solution.

4.3 Determination of the radius of convergence

The computation of the solution of Navier-Stokes problems by means of a polynomial is only valid at low values of the Reynolds number. At higher values, the polynomial series diverges from the FEM data and thus whatever the degree of the polynom considered. The radius of convergence radius of a power series is determined by the behavior of its coefficients at infinity. Since the values of the permeability coefficients depends on R the radius of the cylinder, the radius of convergence then also depends of R. When the higher order permeability coefficients are very small compared to the first order permeability $\boldsymbol{K}^0$ (that appears in the linear Darcy law), the non linear effects only appears for very large values of the pressure gradient. This is observed particularly for $R = 0.45$ or $R = 0.49$ on figures 5 and 6. Conversely, these non linear effects are observed for lower values of the pressure gradient (see the cases $R = 0.05$ and $R = 0.25$ on figures 3 and 4).
There is various possibilities to evaluate numerically the convergence radius of the polynomial series. When only the component J_1 is applied to the system

Accepted Manuscript

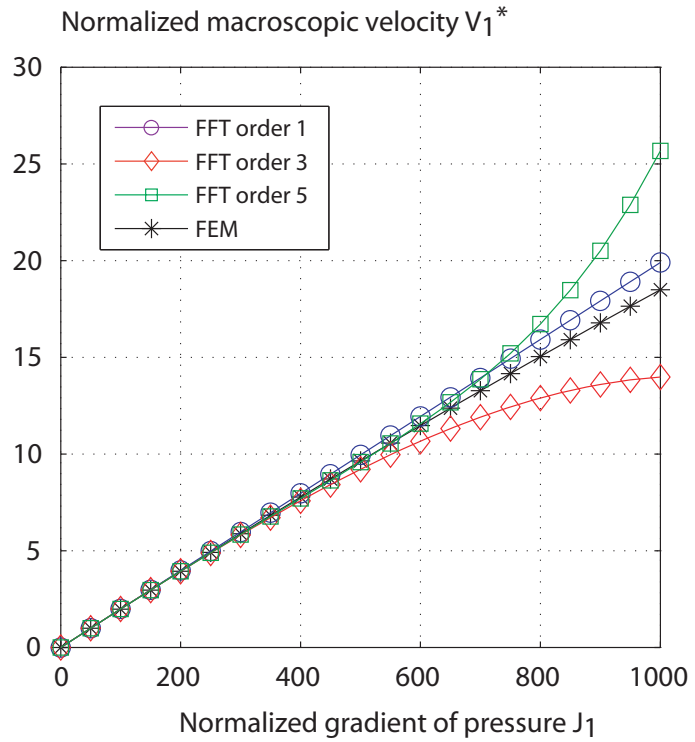

Fig. 4 Variations of the normalized macroscopic velocity V_1^* as function of the normalized macroscopic pressure gradient J_1 for the array of cylinder with circular cross section with radius $R = 0.25$. Comparison between the first order, third order, fifth order approximation and the (FEM based) full solution.

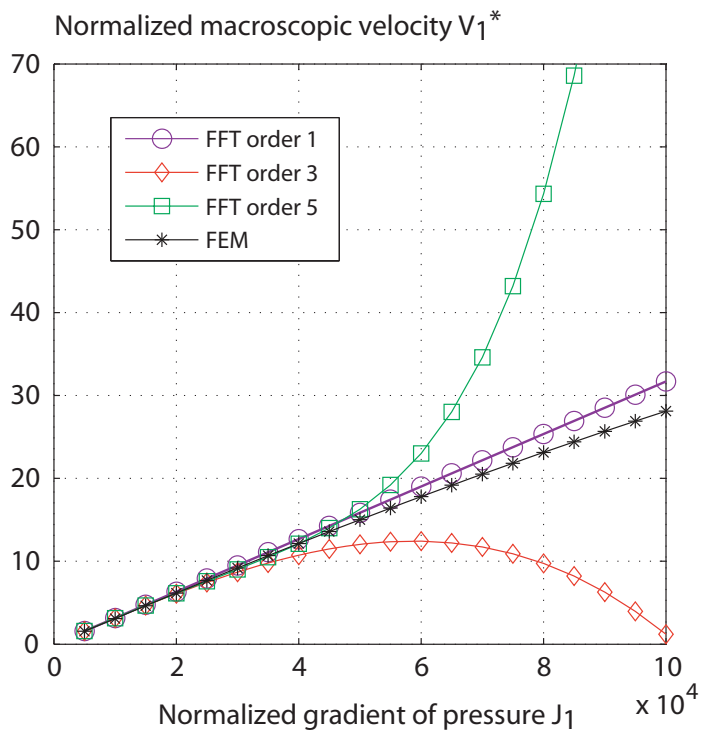

Fig. 5 Variations of the normalized macroscopic velocity V_1^* as function of the normalized macroscopic pressure gradient J_1 for the array of cylinder with circular cross section with radius $R = 0.45$. Comparison between the first order, third order, fifth order approximation and the (FEM based) full solution.

Accepted Manuscript

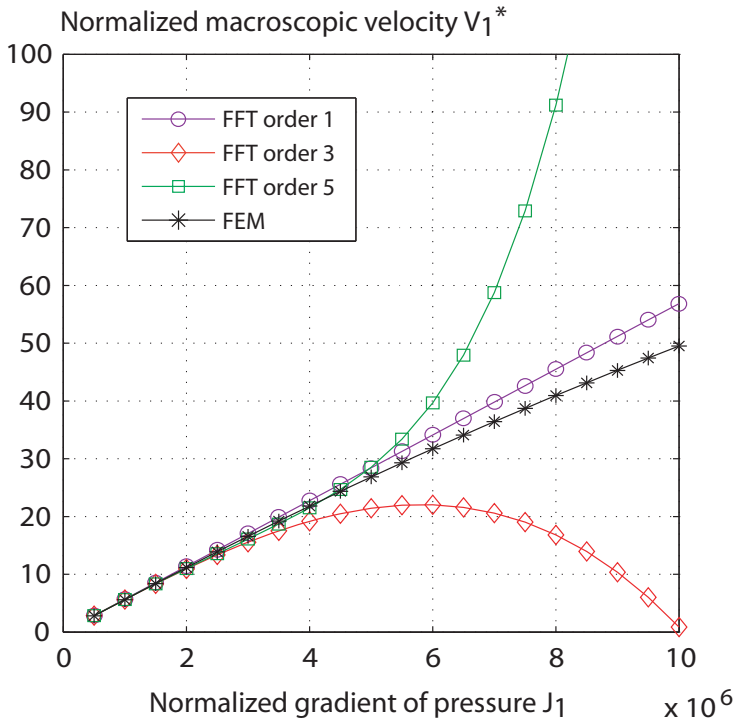

Fig. 6 Variations of the normalized macroscopic velocity V_1^* as function of the normalized macroscopic pressure gradient J_1 for the array of cylinder with circular cross section with radius $R = 0.49$. Comparison between the first order, third order, fifth order approximation and the (FEM based) full solution.

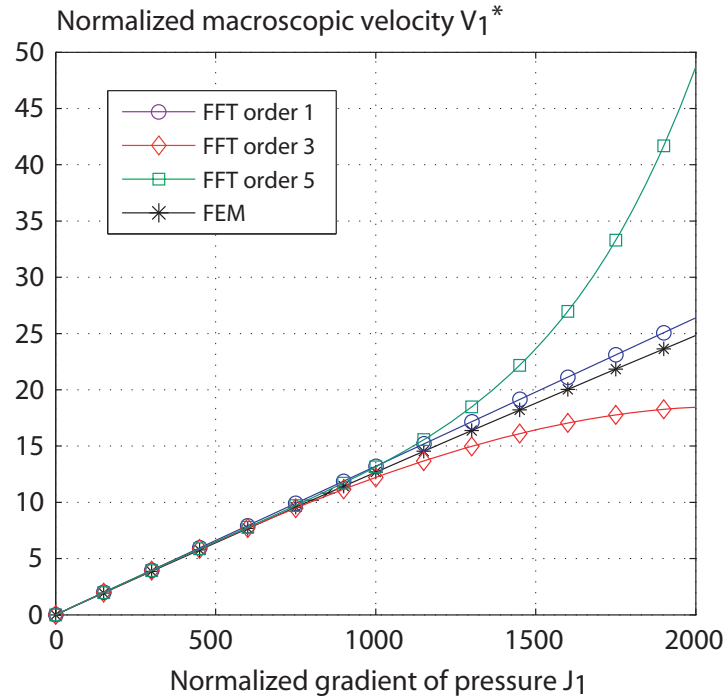

Fig. 7 Variations of the normalized macroscopic velocity V_1^* as function of the normalized macroscopic pressure gradient J_1 for the array of cylinder with rectangular cross section with $a = h/2$. Comparison between the first order, third order, fifth order approximation and the (FEM based) full solution.

Accepted Manuscript

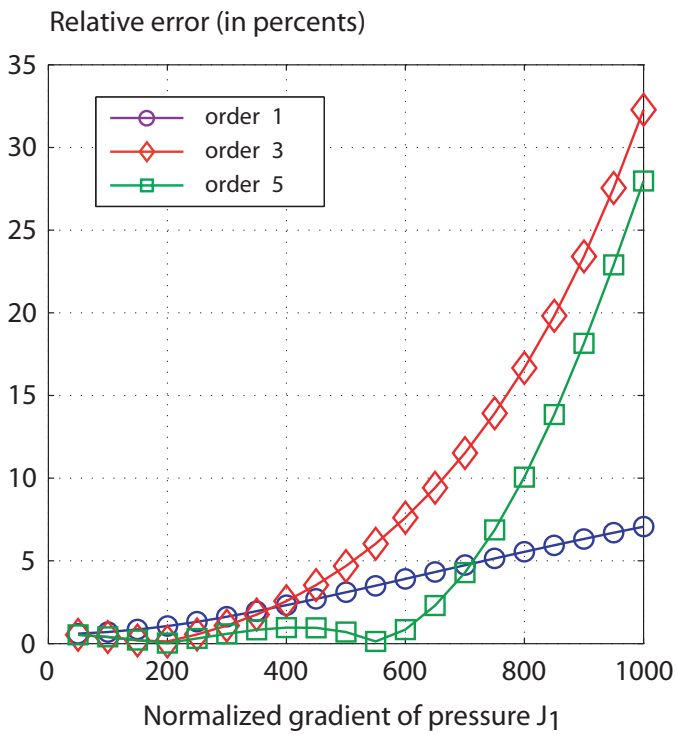

Fig. 8 Relative error (in percents) between polynomial approximation and the solution of full Navier-Stokes equation.

(we put $J_2 = 0$), the series can be put into the form:

$$V_1^* = J_1(c_0 + c_1 J_1^2 + c_2 J_1^4 + ...) \tag{56}$$

where $c_0 = k_0$, $c_1 = k_2 + k_2'$, $c_2 = k_4 + k_4' + k_4''$ etc. We propose to use the Domb and Sykes [12] formula to evaluate the convergence radius of the polynomial series. The convergence radius of the series $c_0 + c_1 x + c_2 x^2 + c_3 x^3 + ...$ could be evaluated by the formula

$$r = \lim_{n \to +\infty} \frac{c_{n-1}}{c_n} \tag{57}$$

Since the sign of the coefficients c_n alternate between 1 and -1, the last formula is then negative. In that case, the value of r must be interpreted as the opposite of the radius of convergence.

Accepted Manuscript

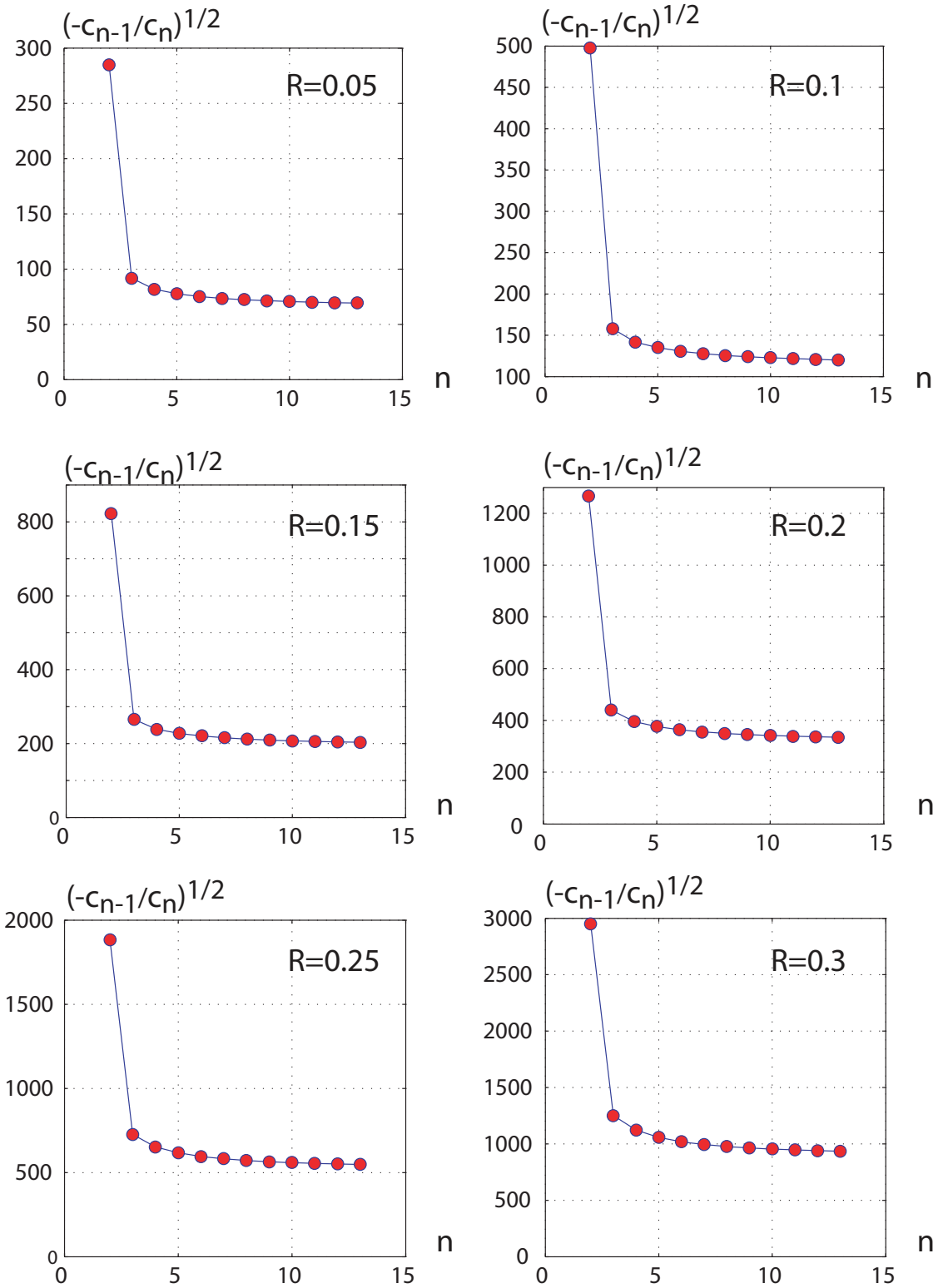

Fig. 9 Domb-Sykes plots giving the value of $(c_{n-1}/c_n)^{-1/2}$ as function of n for various values of the radius of the cylinder $R = 0.05$, $R = 0.1$, $R = 0.15$, $R = 0.2$, $R = 0.25$ and $R = 0.3$.

Moreover, since the series in (56) is in power of J_1^2 the convergence radius for J_1 is given by:

$$\mathcal{R}_J = \lim_{n \to +\infty} \sqrt{-\frac{c_{n-1}}{c_n}} \tag{58}$$

where $\mathcal{R}_J$ is the convergence radius of the series (56). Also, the convergence of the series could be expressed in term of the dimensionless macroscopic velocity V_1^* and is denoted $\mathcal{R}_V$. By computing $\mathcal{R}_J$ and $\mathcal{R}_V$ numerically, and considering that $V_1^* = \mathcal{R}_e$, the limit of the expansion series method can be also expressed in term of the pore Reynolds numbers as follows:

$$\mathcal{R}_e \leq \mathcal{R}_V \tag{59}$$

Practically, the estimation of the convergence radius can be performed by computing the variations of $(-c_{n-1}/c_n)^{1/2}$ as function of n. This is done of figure 9. It must be recalled that we do not analyse the radius of convergence of an analytical function but a numerical function that is determined by solving a hierarchy of elementary problems. The radius of convergence is determined by computing the first 13 coefficients of the series in (58). This requires the resolution of the first 26 elementary problems since the problems of odd order provides zeros coefficients in the expansion series and only the elementary problems of even number provides the coefficients c_0, c_1, c_2, etc in relation (56). The values $(-c_{n-1}/c_n)^{1/2}$ as function of n are represented for various values of the radius R of the cylinder on figure 9. In each case, a good convergence of the series $(-c_{n-1}/c_n)^{1/2}$ is observed and an accurate value of the limit in (58) can be determined after a few number of iterations. We have evaluated the radius of convergence by taking the value of $(-c_{n-1}/c_n)^{1/2}$ for $n = 13$.
Once $\mathcal{R}_J$ and $\mathcal{R}_V$ are determined the results are also interpreted in term of the limit for the pore Reynolds number $\mathcal{R}_e$. For instance, on figure 10, we first represent the limit $\mathcal{R}_J$ as function of the radius R of the cylindric solid. It is observed that the dependence with R is almost linear in the log frame. This proves that the radius of convergence is the largest for almost touching cylinders. Conversely, for small cylinders, the radius of convergence is also small and the non linear effect are expected to be important.
From figure 10, it is possible to determine the limit of the expansion series approach for the applied pressure gradient. As for example, considering water, the values of the dynamic viscosity and mass density are $\mu = 10^{-3} Pa.s$ and $\rho = 1kg/m^3$ at room temperature. We also assume that the distance between two neighboring cylinders is 1 millimeter (that corresponds to the size of the unit cell, $h = 1$). Consequently, we have $G_1 = J_1$. The figure 10 then provides the limit of the applied pressure gradient G_1 in Pa/m for which the expansion into polynomial series of the Navier-Stokes problem is possible. Considering the flow of air, the dynamic viscosity is $1.8 \times 10^{-5} Pa.s$ and the masse density is $\rho = 1.3kg/m^3$, it follows that $G_1 = 0.27 J_1$. The application of results on figure 10 for air must be applied after the multiplication by the factor 0.27.
On figure 10, we represent the limit of the expansion series for the Reynolds number $\mathcal{R}_e$ as function of the radius R of the cylinders. It is observed that

Accepted Manuscript

the limit for $\mathcal{R}_e$ is quasi independent of R and is approximatively equal to 9.5. Similar results are displayed on figure 12 for the regular array of cylinders with squared cross sections. Again, it is observed that the limit for the Reynolds number is almost independent of the size of the squares (denoted by a) and the expansion series is valid for, approximatively, $\mathcal{R}_e \leq 7.5$.

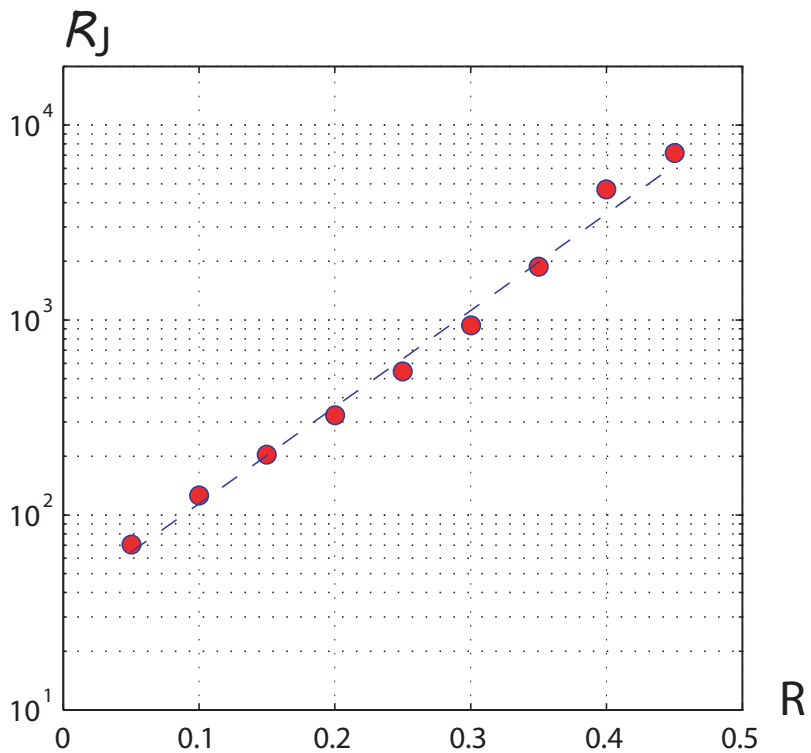

Fig. 10 Convergence radius of the polynomial series for J_1 as function of the radius R of the rigid cylinders with circular crossed sections.

Accepted Manuscript

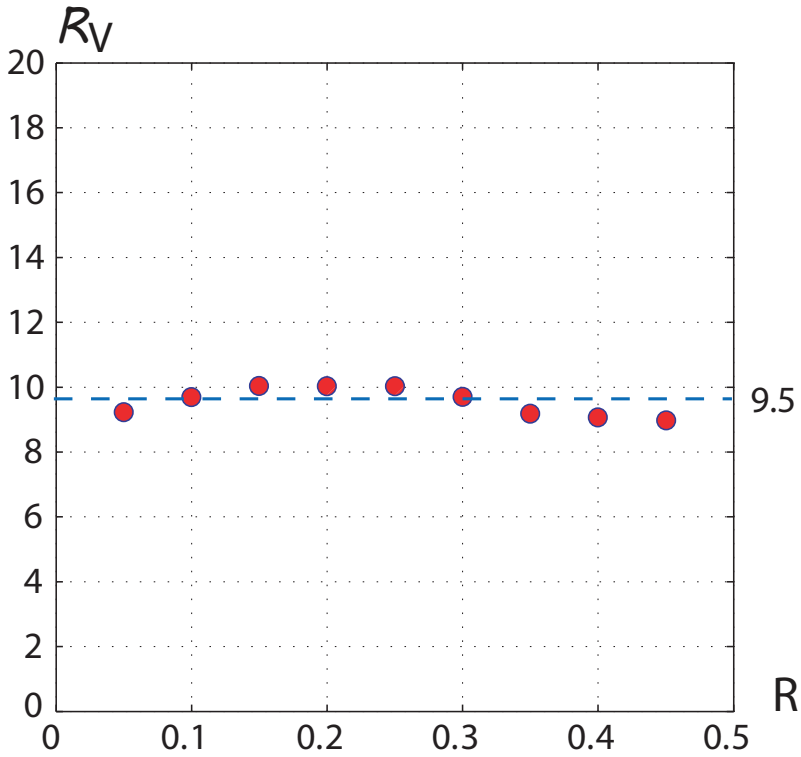

Fig. 11 Convergence radius of the polynomial series for $V_1^* \equiv \mathcal{R}_e$ as function of the radius R of the rigid cylinders with circular crossed sections.

Accepted Manuscript

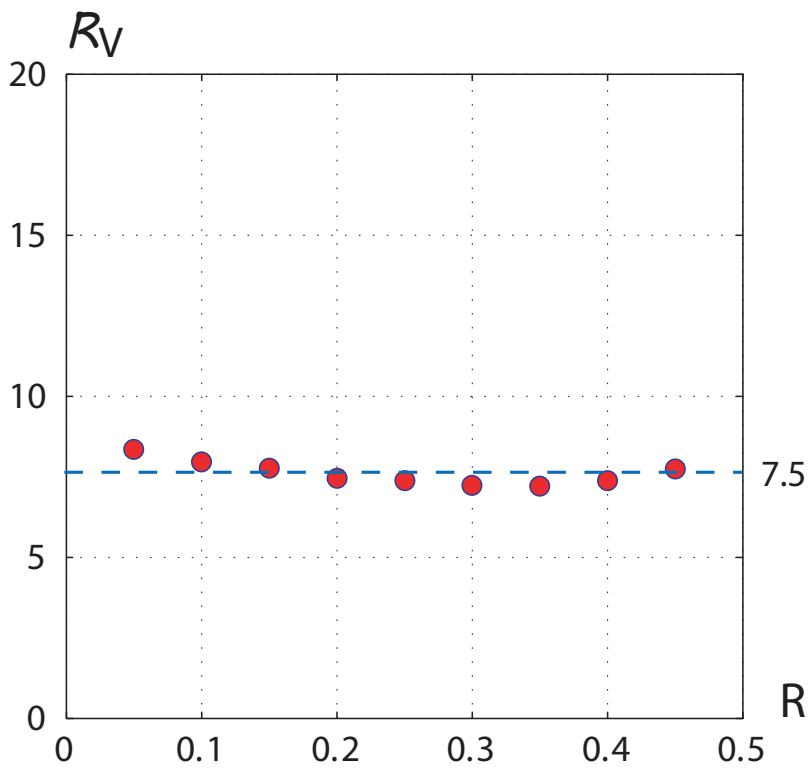

Fig. 12 Convergence radius of the polynomial series for $V_1^* \equiv \mathcal{R}_e$ as function of the dimension size a of the rigid cylinders with squared crossed sections.

4.4 Polynomial approximation of FEM results

By plugging the finite element data, it is obviously possible to approximate the solution by a polymonial into the form given by (51). For instance, such an approximation is performed on figure 13 using a third order or a fifth order polynomial and the least square method for the data fitting. It is observed that the polynomial approximation reproduce the FEM data but fails out of the interval of interpolation that is inherent with the use of polynomials. Additionally, note that the coefficients obtained by fitting the FEM data are quite different that ones computed by the homogenization approach based on asymptotic expansions. The non linear filtration law shown on figure 13 has

Accepted Manuscript

been approximated with a polynomial containing terms of odd degree. The representation of the non linear Darcy law with polynomial functions of odd degree is exact at low Reynolds number but there are just considered as an approximation when these are used in the range of higher values of pressure gradient. There is in fact no arguments for not using polynomial functions of even degree. More generally, the use of vector-valued polynomial functions for the approximation of the non linear filtration law reproduce correctly the dependence between the velocity and the pressure gradient. The expansion

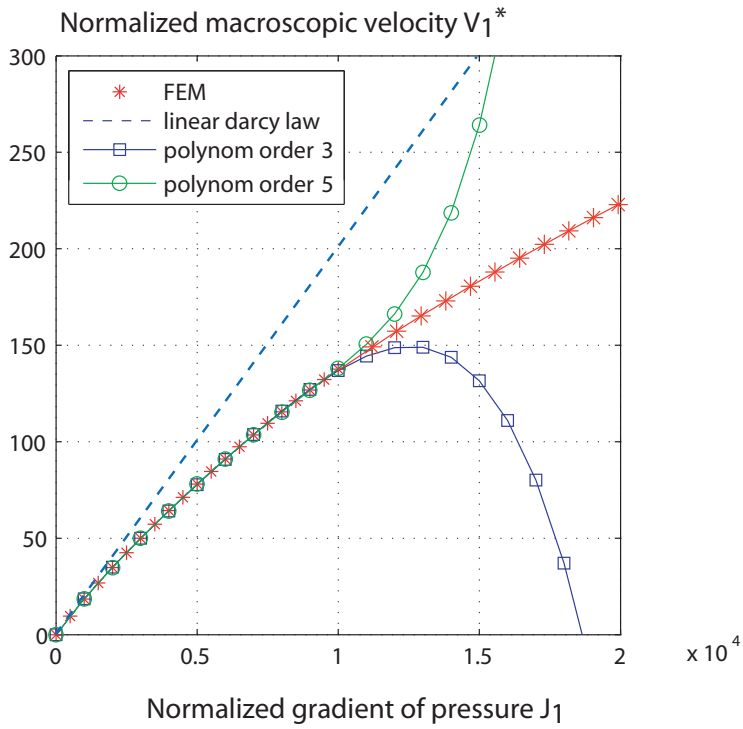

Fig. 13 Approximation of the FEM solution using polynomials.

method is really attractive because it consists in solving linear problems for the unit cell and furthermore the use of the FFT algorithm is numerically interesting for their computation. However, the results show that this approach is not able to reproduce adequately the non linear effects in the range of pressure gradient for which it becomes significant. In other hand, the full Navier-Stokes problem cannot be solved by the FFT method presented in this paper due to the nonlinearity. The technique based on FFT is interesting for computing the problems with high dimensions, that is the case, for example, when the microstructure is defined by digital images which come from microtomography. The development of such type of algorithms for computing the solution to Navier-Stokes equations is obviously of great interest in the field of homogenization. Note that non linear homogenization problems has been tackled with the FFT technique for various application to composite materials, see for example [28, 24, 26]. However, in these studies, the non linearity comes from the strain-stress relation that is quite different. It follows that the computation of

Accepted Manuscript

the Navier-Stokes problem with FFT must be handled with the development of new algorithms.

5 Conclusion

In this work, we have provided a numerical analysis of non linear correction's to Darcy law. These non linearities are accounted in the framework of periodic homogenization of porous media in which the flow is described by the Navier-Stokes equations with periodicity conditions on the boundary of the unit cell. On the basis of earlier theoretical studies, the solution is approximated by a Taylor expansion series that leads to solving a chain of elementary Stokes-type problems which are must easier than solving the full Navier Stokes equation. A Fast numerical algorithm based on FFT has been formulated to compute the solution of each Stokes auxiliary problems and the higher order permeability tensors. The capacity of this approach to reproduce the non linear effects has been thereafter investigated numerically in the case of the flow through an array of aligned cylinders with circular and squared cross sections and compared to direct FEM resolution of Navier Stokes equation. The results show that the range polynomial filtration law is only applicable within a limited range of velocity for which the correction to Darcy law is in fact very small. In a larger range, the polynomial approximation fails to reproduce the non linear correction to Darcy law. Moreover, while the FEM solution can be approximated by a polynomial equation, the identification of the constitutive parameters significantly differs from that delivered by the resolution of the successive elementary Stokes problems. Future work will focus on the development on FFT based numerical approach for the resolution of full Navier-Stokes problem.

References

1. Adler, P.M., Malevich, A.E., Mityushev, V.V.: Nonlinear correction to DarcyŠs law for channels with wavy walls. Acta Mechanica. 224(8), 1823-1848 (2013)
2. Ahmad, N.: Physical properties of porous medium affecting laminar and turbulent flow of water. Ph. D. Thesis, Colorado State University, Fort Collins (1967)
3. Allaire, G.: Homogenization of the Stokes flow in connected porous medium. Asymptotic Anal. 3, 203Ű222 (1989)
4. Auriault, J.-L., Geindreau, C., Boutin, C.: Filtration Law in Porous Media with Poor Separation of Scales. Transport in Porous Media 60(1), 89-108 (2005)
5. Auriault, J.-L. and Boutin, C. and Geindreau, C.: Homogenization of coupled phenomena in heterogenous media, John Wiley & Sons, 2010.
6. Bahloff, M., Mikelic, A., Wheeler, M.F.: Polynomial filtration law for low Reynolds number flows through porous media. Transport in Porous Media. 81, 36-60 (2010)
7. Barrère, J.: Modélisation des écoulements de Stokes et Navier-Stokes en milieu poreux. Doctoral thesis at Université de Bordeaux I (1990)
8. Bourgeat A., MaruŽic- Paloka E., Mikelic A.: Weak non-linear corrections for DarcyŠs Law. M3 AS Math. Models Methods Appl. Sci. 6(8), 1143Ű1155 (1996)
9. Chen Z., Lyons S.L., Qin G.: Derivation of the Forchheimer law via homogenization. Transp. Porous Med. 44, 325Ű335 (2001)
10. Chauveteau, G., Thirriot, C.: Régimes d'écoulement en milieu poreux et limite de la loi de Darcy. La Houille Blanche. 2, 141Ű148 (1967)

Accepted Manuscript

11. Darcy, H.: Les Fontaines Publiques de la Ville de Dijon, Victor Dalmond (1856)
12. Domb, V., Sykes, M.F.: Use of series expansions for the ising model susceptibility and excluded volume problem. J. Maths. Phys. 7, 2-63 (1961)
13. Edwards, D.A., Shapiro, M., Bar-Yoseph, P., Shapira, M.: The influence of Reynolds number upon the apparent permeability of spatially periodic arrays of cylinders. Phys. Fluids A. 2 (1990)
14. Firdaouss M., Guermond J.L., Le Quéré P.: Nonlinear corrections to DarcyŠs law at low Reynolds numbers. J. Fluid Mech. 343, 331Ű350 (1997)
15. Forchheimer, P.: Wasserbewegung durch Boden, VDIZ 45, 1782-1788 (1901)
16. Giorgi, T.: Derivation of the Forchheimer law via matched asymptotic expansions, Transport in Porous Media 29, 191-206 (1997)
17. Kim, B.Y.K.: The resistance to flow in simple and complex porous media whose matrices are composed of spheres. M.Sc. thesis, University of Hawaii at Manoa (1985)
18. Kim, J., Lee, J., Lee, K.C.: Nonlinear correction to Darcy's law for a flow through periodic arrays of elliptic cylinders. Physica A: Statistical Mechanics and its Applications. 293(1):13-20 (2001)
19. Lasseux, D., Abbasian Arani, A.A. and Ahmadi A. On the stationary macroscopic inertial effects for one phase flow in ordered anddisordered porous media, Phys. Fluids, 23, 073103 (2011)
20. Lindquist, E.: On the flow of water through porous soils. Premier Congrès des Grands Barrages, Stockholm 5, 81Ű101 (1933)
21. Ly, H.-B.: Computation of permeability of complex 3d porous materials and digital images with FFT method. To appear.
22. Mei C.C., Auriault J.-L.: The effect of weak inertia on flow through a porous medium. J. Fluid Mech. 222, 647Ű663 (1991)
23. MacDonald, I. F., El-Sayed, M. S., Mow, K. and Dullien, F. A. L.: Flow through porous media: the Ergun equation revisited, Indust. Chem. Fundam. 18, 199-208 (1979).
24. Michel J. C., Moulinec H., Suquet P. A computational scheme for linear and non-linear composites with arbitrary phase contrast. *Int. J. Numer. Meth. Engng.* 2001, vol. 52, pp. 139-160.
25. Monchiet V., Bonnet G., Lauriat G. A FFT-based method to compute the permeability induced by a Stokes slip flow through a porous medium. *Comptes Rendus Mécanique.* Vol. 337(4), pp. 192-197 (2009)
26. Monchiet V., Bonnet G. Numerical homogenization of non linear composites with a polarization-based FFT iterative scheme. *Comput. Mater. Science.* Vol. 79, pp. 276-283, 2013.
27. Moulinec H. and Suquet P. A fast numerical method for computing the linear and nonlinear mechanical properties of composites. *C. R. Acad. Sci.* 1994, vol. 318 (11), pp. 1417-1423.
28. Moulinec H. and Suquet P.
A numerical method for computing the overall response of nonlinear composites with complex microstructure. *Comput. Methods. Appl. Mech. Engrg.* 1998, vol. 157, pp. 69-94.
29. Nguyen T.-K., Monchiet V., Bonnet G. A Fourier based numerical method for computing the dynamic permeability of porous media. *European Journal of Mechanics B/fluids.* Vol. 37, pp. 90-98 (2013)
30. Peszynska, M., Trykozko, A., Augustson, K.: Computational Upscaling of Inertia Effects from Porescale to Mesoscale. Computational Science Ű ICCS 2009. 5544, 695-704 (2009)
31. Rasoloarijaona M., Auriault J.-L.: Non-linear seepage flow through a rigid porous medium. Eur. J. Mech. B Fluids 13(2), 177Ű195 (1994)
32. Skjetne, E., Thovert, J.-F., Adler, P.M.: High-velocity flow in spatially periodic porous. Ing (Ed.), Norwegian University of Science and Technology, 9Ű82 (1995).
33. Skjetne E., Auriault J.L.: New insights on steady, non-linear flow in porous media. Eur. J. Mech. B Fluids 18(1), 131Ű145 (1999)
34. Sunada, D.K.: Laminar and turbulent flow of water through homogeneous porous media. PhD dissertation, University of California at Berkeley (1965)
35. Tartar, L.: Compensated compactness and applications to PDEs, in: J. Knops (ed.), Nonlinear Analysis and Mechanics, Heriot-Watt Symposium, vol. IV, Research Notes in Math. Pitmann, London, pp. 136-212 (1979)

Accepted Manuscript

36. Whitaker, S.: Flow in porous media I: A theoretical derivation of Darcy's law. Transport in Porous Media 1(1), 3-25 (1986)
37. Wodie, J.-C. and Levy, T.: Correction non lineaire de la Loi de Darcy, C. R. Acad. Sci. Paris, Serie II 312, 157-161 (1991)
38. Zermatten, E., Schneebeli, M., Arakawa, H. and Steinfeld, A. Tomography-based determination of porosity, specific area and permeability of snow and comparison with measurements. Cold Regions Science and Technology, 97, 33-40 (2014).
39. Zheng, Q.-S.:Two-dimensional tensor function representation for all kinds of material symmetry. Proc. R. Soc. Lond., 443(1917), 127-138 (1993)

Accepted Manuscript